Article

Patterns

Data-driven evaluation of electric vehicle energy consumption for generalizing standard testing to real-world driving

Graphical abstract

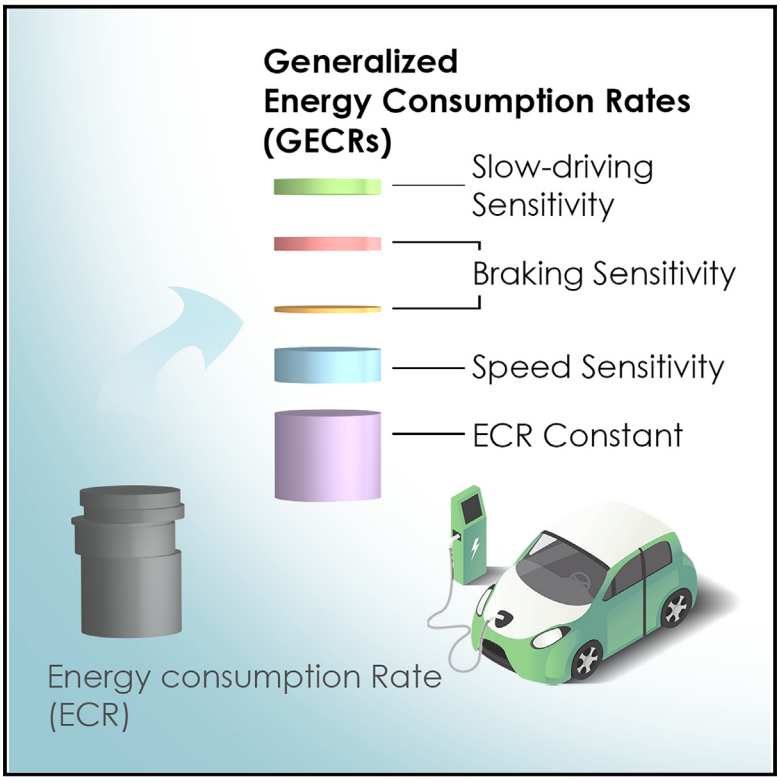

Highlights

- We propose a generalizable energy consumption evaluation method for BEVs
- Our method is compatible with the existing test procedures, enabling standardization
- Rigorous driving behaviors with high interpretability are characterized
- The method could promote public awareness of electric vehicle energy consumption

Authors

Xinmei Yuan, Jiangbiao He, Yutong Li, ..., Hui Zhang, Yucheng Jin, Long Sun

Correspondence

yuan@jlu.edu.cn

In brief

An approach for comprehensively evaluating battery electric vehicle energy consumption is presented here. By incorporating a data-driven approach into the standard testing procedure, the evaluation results are generalizable to various driving conditions, resolving the inconsistency between conventional standard testing and real-world driving. This approach shows great potential for promoting the public understanding and acceptance of electric vehicles while also providing a fundamental model for more reliable energy-consumption assessments for future sustainable transportation.

Yuan et al., 2024, Patterns 5, 100950
April 12, 2024 © 2024 The Author(s).
https://doi.org/10.1016/j.patter.2024.100950

CellPress

Patterns

CellPress
OPEN ACCESS

Article

Data-driven evaluation of electric vehicle energy consumption for generalizing standard testing to real-world driving

Xinmei Yuan,[1,2,3,8,*] Jiangbiao He,[4] Yutong Li,[5] Yu Liu,[1,2] Yifan Ma,[1,2] Bo Bao,[1,2] Leqi Gu,[1,2] Lili Li,[3] Hui Zhang,[6] Yucheng Jin,[6] and Long Sun[7]

[1]State Key Laboratory of Automotive Simulation and Control, Jilin University, Changchun 130025, China
[2]College of Automotive Engineering, Jilin University, Changchun 130025, China
[3]Sichuan Energy Internet Research Institute, Tsinghua University, Chengdu 610299, China
[4]Department of Electrical & Computer Engineering, University of Kentucky, Lexington, KY 40506, USA
[5]Department of Aerospace Engineering, University of Michigan, Ann Arbor, MI 48109, USA
[6]Changchun Automotive Test Center Co., Ltd., Changchun 130011, China
[7]CATARC Automotive Test Center (Tianjin) Co.,Ltd., Tianjin, 300300, China
[8]Lead contact
*Correspondence: yuan@jlu.edu.cn
https://doi.org/10.1016/j.patter.2024.100950

THE BIGGER PICTURE With the rapidly increasing market penetration of battery electric vehicles (BEVs) worldwide, having reliable and publicly available information on BEV energy consumption is critical. The disparity between standard-tested and real-world BEVs' actual energy consumption, however, can mislead the low-carbon development of the global automotive industry. To align standard testing with real-world driving, standardizable energy evaluation frameworks should be adaptable to different driving conditions. Such frameworks could then provide publicly available fundamental models for more reliable BEV energy-consumption estimation and benefit broad stakeholders related to eco-driving guidance, carbon assessment, policymaking, vehicle-grid interaction, and intelligent transportation.

SUMMARY

Standard energy-consumption testing, providing the only publicly available quantifiable measure of battery electric vehicle (BEV) energy consumption, is crucial for promoting transparency and accountability in the electrified automotive industry; however, significant discrepancies between standard testing and real-world driving have hindered energy and environmental assessments of BEVs and their broader adoption. In this study, we propose a data-driven evaluation method for standard testing to characterize BEV energy consumption. By decoupling the impact of the driving profile, our evaluation approach is generalizable to various driving conditions. In experiments with our approach for estimating energy consumption, we achieve a 3.84% estimation error for 13 different multiregional standardized test cycles and a 7.12% estimation error for 106 diverse real-world trips. Our results highlight the great potential of the proposed approach for promoting public awareness of BEV energy consumption through standard testing while also providing a reliable fundamental model of BEVs.

INTRODUCTION

Battery electric vehicles (BEVs) significantly reduce emissions from road transportation, where conventional combustion-engine-based vehicles have long been the leading contributors to global greenhouse gas emissions in the transportation sector.[1–3] Considering the energy crisis and emission concerns, BEV energy consumption has become an increasingly critical factor to consider when addressing climate change and urban environmental concerns in sustainable transportation.[4–8] The energy-consumption rate (ECR), i.e., the amount of energy consumed per unit driving distance, has been widely used to evaluate the energy consumption of BEVs. For standardization, the ECR is determined under specific test conditions, namely, the standardized driving cycle, which is considered the most representative driving profile. This paradigm has been used to promote

This is an open access article under the CC BY-NC-ND license (http://creativecommons.org/licenses/by-nc-nd/4.0/).

transparency and accountability within the automotive industry since the late 1960s.[9] However, as the most significant influencing factor of standard evaluations of BEV energy consumption, the standardized driving cycle has become the primary development focus for most automotive manufacturers,[10] with diverse real-world driving conditions potentially overlooked during the development phase. As a result, the standardized-cycle-tested ECR has been increasingly criticized because it inaccurately reflects real-world driving conditions,[11,12] leading to notable dissatisfaction and anxiety among consumers.[13,14] Moreover, this discrepancy has created significant controversy in carbon evaluations of BEVs. For instance, in Letmathe and Suares,[15] an uplift factor of 46% was adopted to compensate for the underestimated real-world energy consumption in standardized testing. Conversely, Desreveaux et al.[16] concluded that standard driving cycles overestimate the real-world driving energy consumption of BEVs, thereby reducing the potential benefits of BEVs in terms of global warming potential by 50%. Consequently, the unreliability of existing standard testing procedures poses a severe challenge for policymakers, engineers, and academic researchers in developing reliable energy and carbon emission models to address future environmental goals.

Several studies have empirically corrected the mean real-world biases of standard ECR evaluation results with scaling factors to obtain more realistic energy-consumption evaluation results that better reflect real-world driving,[17–19] while other studies have focused on developing more representative test cycles for different cities and regions (for more details, see Note S1). However, corrected ECRs and cycle-tested ECRs are still constant, while the ECRs of BEVs in the real world vary significantly (for more details, see Note S2). Thus, ECRs determined via empirical correction or highly representative cycle tests still cannot be generalized to real-world driving.

Extensive studies have been performed to obtain generalizable BEV energy-consumption data through modeling approaches. Notably, physically based models, e.g., TripEnergy, have been developed and widely used.[20,21] Although physically based models encompass the underlying mechanisms of BEV energy consumption and can achieve high accuracy, they are rarely adopted for standard evaluation. This is primarily due to the challenge of accurately calibrating the model parameters within the context of standardized testing, which requires simplicity and accessibility. Data-driven approaches, also known as artificial intelligence methods,[22] include neural networks,[23] deep neural networks,[24] fuzzy clustering,[25] decision trees,[26] ensemble learning,[26,27] and linear models[23,28] and have been adopted to estimate BEV energy consumption. Although these models do not require specialized expertise and can accurately estimate BEV energy consumption under various driving conditions, they have rarely been employed in standard testing. This is primarily because their complex algorithms and underlying mechanisms pose challenges in fulfilling the interpretability criteria for standard testing; therefore, transparent and easily understandable methodologies are needed to ensure consistent and reliable results. Additionally, because of time limitations and cost concerns associated with official standard tests, the amount of data collected during standard testing is insufficient for advanced machine learning models.[29] In brief, the existing modeling approaches can provide generalized estimates of BEV energy consumption, but they usually fail to meet the requirements of standard testing.

We address standard testing here because of its significance in terms of public awareness regarding BEV energy consumption compared with other approaches. Other approaches typically require additional testing or parameters specific to a particular BEV model. However, the accessibility of such testing or parameters for the majority of BEV models is limited, thus hindering their widespread implementation. In contrast, standard testing is mandatory for all BEV models, providing an inherent opportunity for characterizing BEV energy consumption. Considering the global trend toward decarbonization in the transportation sector, there is an increasing need for reliable and publicly available information on BEV energy consumption for all different BEV models. Accurate publicly available energy-consumption information on BEVs can increase public awareness of BEV energy consumption and eco-driving activities, reduce range anxiety, and contribute to advancing energy-consumption regulations to promote the comprehensive optimization of BEVs. Moreover, this information holds significant value across a broad spectrum of research fields that require accurate energy-consumption estimates and optimization, such as for carbon assessments, vehicle-grid interactions, and route planning. As a result, establishing an improved evaluation framework that comprehensively captures the energy-consumption characteristics of BEVs while ensuring reliable and standardizable testing designs is crucial.

In this work, we present a physically interpretable data-driven approach to characterize the energy consumption of BEVs and propose generalized ECRs (GECRs) as an alternative to the ECR for standard evaluation. Since GECRs decouple driving conditions from energy consumption, they reflect the inherent energy-consumption characteristics of BEVs, making them adaptable to a wide range of driving profiles. We experimentally validated our approach in both laboratory and real-world environments. In the laboratory tests, the GECRs were characterized and evaluated for different test cycles, including standardized driving cycles for various road types in different regions and constant-speed segments (CSSs). Our results showed that the mean absolute percentage error (MAPE) of the GECRs was 3.84% for a set of 13 laboratory test cycles, approximately five times less error than that based on existing standard results. Additionally, a MAPE of 7.12% was achieved for 106 driving trips in our real-world tests, further validating the generalizability of the GECRs. The results highlight the improved generalizability and physical interpretability of our approach while confirming its compatibility with existing standards. These findings demonstrate the great potential of our approach for enhancing existing standards and significantly reducing the discrepancy between standard testing and real-world driving.

Driving features

Feature selection is a key technique for data-driven models.[30] The incorporation of a limited number of physically rational features is particularly critical when applying data-driven approaches in standard evaluation procedures. Although the relationship between energy consumption and driving profiles is complex, the energy consumption of various components is correlated throughout different energy transfer paths. These correlations can be used to simplify the relationship between energy

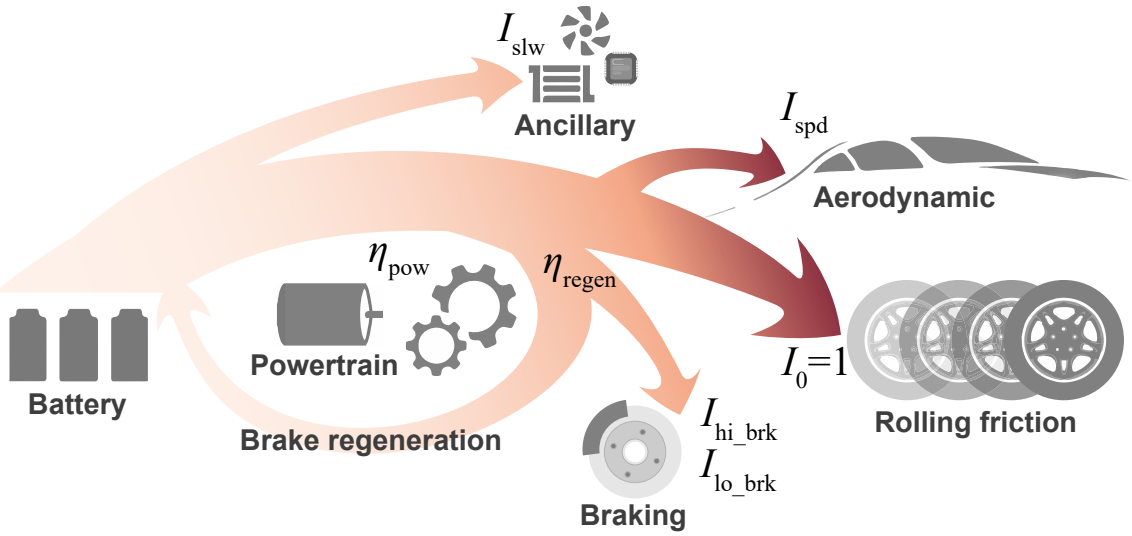

Figure 1. Energy flowchart of a BEV

The energy flow is represented by the red arrows. The energy flows from the battery and eventually dissipates, as shown by the gradually deepening hue. Specifically, as the electric energy flows out of the battery, part of the energy is used to directly power the ancillaries and the remaining energy is consumed by aerodynamic resistance, rolling resistance, and braking through the electric motor and drivetrain, with some of the braking energy flowing back into the battery through the electric motor and drivetrain via regenerative braking.

consumption and the driving profile. During a BEV driving cycle, electric energy flows out of the battery through different paths, consisting of power electronics, electric motors, and drivetrains, and eventually dissipates as one of four types of physically independent loss (final work): rolling friction loss, aerodynamic loss, braking loss, or ancillary loss (pumps, fans, lighting, infotainment, and microcontrollers) (Figure 1). From this perspective, the energy consumption throughout the energy transfer path can be simplified into two parts: the final work performed by the energy flow and the efficiency of the energy flow, which is approximately proportional to the final work performed.

Based on this model, the energy consumption of a BEV is determined primarily based on the four types of final losses. Other losses can be attributed to energy flow efficiencies, which are approximately proportional to the four final losses. As a result, we defined driving features based on the relationships between the final losses and the driving profile, including the speed intensity, high-speed braking intensity, low-speed braking intensity, and slow-driving intensity (detailed in the experimental procedures). The speed intensity represents the driving behavior proportional to the aerodynamic loss, the braking intensities reflect the driving behavior proportional to the braking loss, and the slow-driving intensity is related to driving behavior proportional to ancillary losses. The driving features corresponding to the rolling losses are not defined, because rolling resistance is approximately independent of the driving speed. The braking intensities during high-speed and low-speed braking are defined separately, because regenerative braking (recovery of braking energy with the electric motor operating as a generator) displays distinct characteristics in different speed ranges[31] (effective at high speeds but not at low speeds, as detailed in Note S3). Therefore, the four defined driving features are physically interpretable and decoupled, enhancing the linearity, convergence, and interpretability of our data-driven model.

Generalized energy-consumption rates

Using the defined driving features, we propose GECRs, which consist of the ECR constant, speed sensitivity, high-speed braking sensitivity, low-speed braking sensitivity, and slow-driving sensitivity. The ECR constant corresponds to the constant portion of the ECR, which does not vary with the driving speed, and the speed sensitivity, high- and low-speed braking sensitivities, and slow-driving sensitivity correspond to the ECR components and are proportional to the four driving features (a detailed physical derivation is provided in Note S4).

The GECRs are designed to be characterized through existing standard testing procedures. We compare our approach with current standards[32–34] to demonstrate its high compatibility and improved generalizability. According to the existing standards (Figure 2A), historical driving data are used to obtain real-world driving statistics, and probabilistic approaches such as Markov chains are utilized to generate standardized driving cycles. The evaluation result is based on the ECR of the standardized driving cycle. However, standardized driving cycles are unable to accurately reflect diverse individual behaviors due to their uniqueness and the spatial and temporal limitations of historical data; therefore, standard-test-based ECRs are inconsistent with consumer experience. In our approach (Figure 2B), a similar test procedure is used; however, the driving features of the test cycle are extracted and decoupled from the ECR during the postprocessing of the experimental data. Thus, paired with the driving features of a specific driving profile, GECRs represent the corresponding ECR; therefore, they can be generalized to various users.

In detail (Figure 2C), by introducing a stepwise regression approach, the relationship between the standardized-cycle-tested ECR and the driving features of the standardized cycle is decoupled to obtain the GECRs. The driving features of a specific driving profile are extracted and serve as scaling factors for

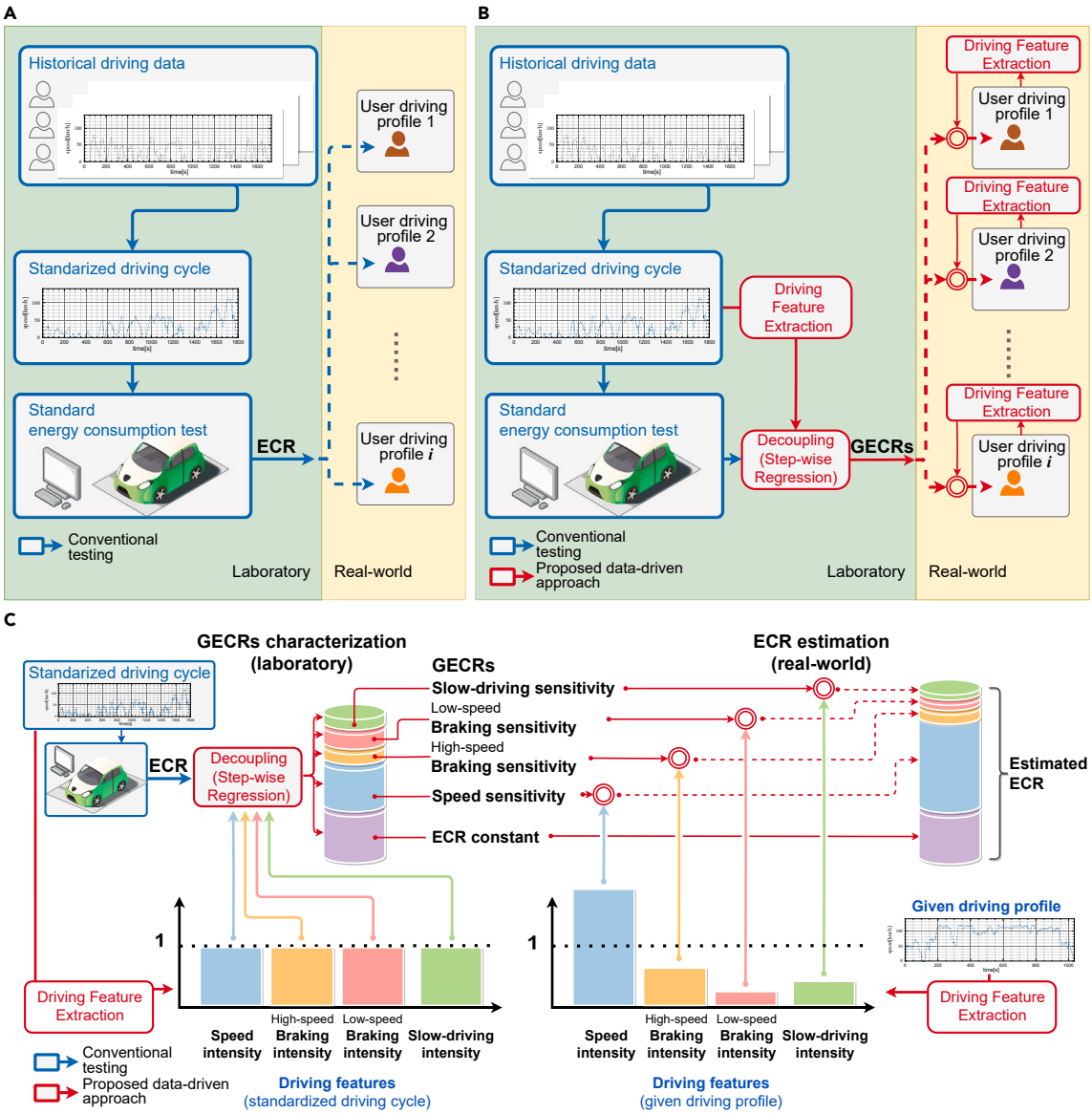

Figure 2. Schematic of the proposed approach

(A) Illustration of the energy-consumption evaluation approach used in the existing standards. The standardized driving cycle is generated based on historical driving data, and the BEVs are tested under repeated standardized driving cycles in a laboratory environment. As an evaluation outcome, the ECR is provided to various users regardless of the users' actual driving profiles.

(B) Illustration of the proposed energy-consumption evaluation approach. An additional driving-feature-extraction module and a driving-feature-decoupling module are added to the evaluation process. With the driving features decoupled from the ECR, the GECRs are obtained rather than the ECR. As a result, the evaluation outcomes can be adapted to different users by pairing the users' real-world driving features.

(C) Illustration of the principle of adapting the GECRs to users' driving profiles. The GECRs are decoupled from the ECR of the standardized test cycle and divided into five parts based on four normalized driving features: speed intensity, high-speed braking intensity, low-speed braking intensity, and slow-driving intensity. The ECR for a user can be estimated as the sum of linearly scaled GECRs based on the driving features of the specific driving profile.

the GECRs. The estimated ECR for the specific driving profile is simply the sum of the rescaled GECRs. As a result, the specific energy-consumption information for different users can be obtained based on individual driving profiles.

In essence, GECRs approximate a linear relationship between a driving profile and the corresponding ECR, thereby representing the inherent energy consumption characteristics of a BEV independent of driving behaviors. Although the linear approximation of GECRs is influenced by the nonlinearity of the powertrain and regenerative braking efficiencies, as well as by various unmodeled factors, the primary nonlinearity in BEV energy consumption from longitudinal dynamics is decoupled based on driving feature selection. Additionally, GECRs are evaluated at the trip scale, but nonlinearity and unmodeled factors are generally reflected by the differences in second-by-second variations, which are usually averaged

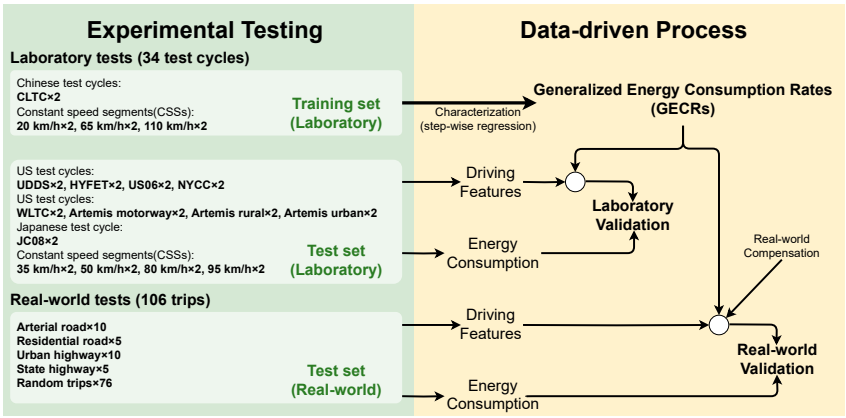

Figure 3. Framework of this study

The framework consists of two primary parts: energy-consumption testing and the data-driven process. The energy-consumption testing includes 34 laboratory test cycles and 106 real-world driving trips. In the data-driven process, the GECRs are characterized from the lab training set. Subsequently, by incorporating the driving features of the laboratory and real-world test sets into the characterized GECRs, the energy-consumption rates of these cycles or trips can be estimated. The generalizability of the GECRs is validated by comparing the estimated energy-consumption rates with measured values.

over a trip; therefore, their impact is significantly reduced in the characterization of GECRs (for a more detailed discussion, see Note S4).

Data generation

The framework of this study is shown in Figure 3. All the data were collected via experimental testing with a Tesla Model 3 (2019 standard range plus, RWD), which has been a mass-produced, globally sold typical BEV model. We characterized the GECRs based on a variant China light-duty-vehicle test cycle (CLTC) procedure, with repeat tests based on the CLTC and three CSSs (Note S5). To validate the generalizability of the characterized GECRs, laboratory and real-world driving tests were performed. In the laboratory tests, nine different standardized driving cycles (used in the United States, Europe, and Japan) and four different CSSs were selected, and the experiments were repeated twice; a total of 26 observations of diverse driving cycles were obtained (Note S6). For the real-world driving tests, 30 trips on six typical routes and 76 random-driving trips, yielding 106 total trips, were recorded (Note S7). The selected routes included state highways, urban highways, arterial roads, and residential roads, and 5 trips on each selected route were recorded to account for the impact of nonroute factors. The random trips were recorded by randomly following cars at various locations.

Overall, our dataset contained data from 34 laboratory test cycles and 106 real-world driving trips. To our knowledge, our dataset is the most comprehensive and highest-quality publicly available dataset for BEV energy-consumption tests; it contains high-resolution driving data from many laboratory test cycles and real-world driving scenarios for the same BEV.

All laboratory tests were performed following the standard energy-consumption test procedure for BEVs,[32–34] and the real-world driving data were recorded via a controller area network (CAN) bus (Note S7). The state-of-charge (SOC) values of the BEVs in the tests were all less than 90%. This is critical, because high SOC values may alter energy consumption characteristics (Note S8). We did not consider the impact of a high SOC in this study because it is small over the full SOC range, and charging the battery to an extreme SOC is not recommended to improve the overall lifespan of the battery. Our ECR calculations were based on the DC discharged energy; however, the AC recharged energy was also recorded, and the corresponding ECRs and GECRs were derived (Note S9).

Table 1. Characterized GECRs

GECR	Value (Wh/km)
ECR constant	66.3
Speed sensitivity	24.9
High-speed braking sensitivity	3.8
Low-speed braking sensitivity	10.6
Slow-driving sensitivity	11.9
Sum of the GECRs (estimated ECR of the CLTC)	117.5

RESULTS

Characterized GECRs

The characterized GECRs are shown in Table 1, where each GECR contributes to the energy consumption corresponding to a driving feature. For example, the ECR constant is 66.3 Wh/km, representing the base ECR that exists constantly regardless of the driving conditions. The speed sensitivity is 24.9 Wh/km, indicating that the BEV consumes 24.9 Wh/km of additional energy for a given unit increase in the normalized speed intensity. The high-speed braking sensitivity is low, which indicates that braking at high speed consumes little energy due to the high braking regeneration efficiency at high speeds (for more details, see Note S3). With the physical interpretability of GECRs, our model quantitatively explains the variations in ECRs for diverse driving profiles. Additionally, by summing the GECRs, an ECR of 117.5 Wh/km for the CLTC is estimated, which is compatible with the existing standard.

Driving feature distribution

The test sets are used to validate the generalizability of the GECRs. The names of the laboratory-tested cycles are briefly explained in Table 3, while more detailed introductions are provided in Note S6. The distribution of their driving features is visualized (Figures 4A and 4B) to show the driving feature space, which was broadly probed in laboratory tests. The test cycles

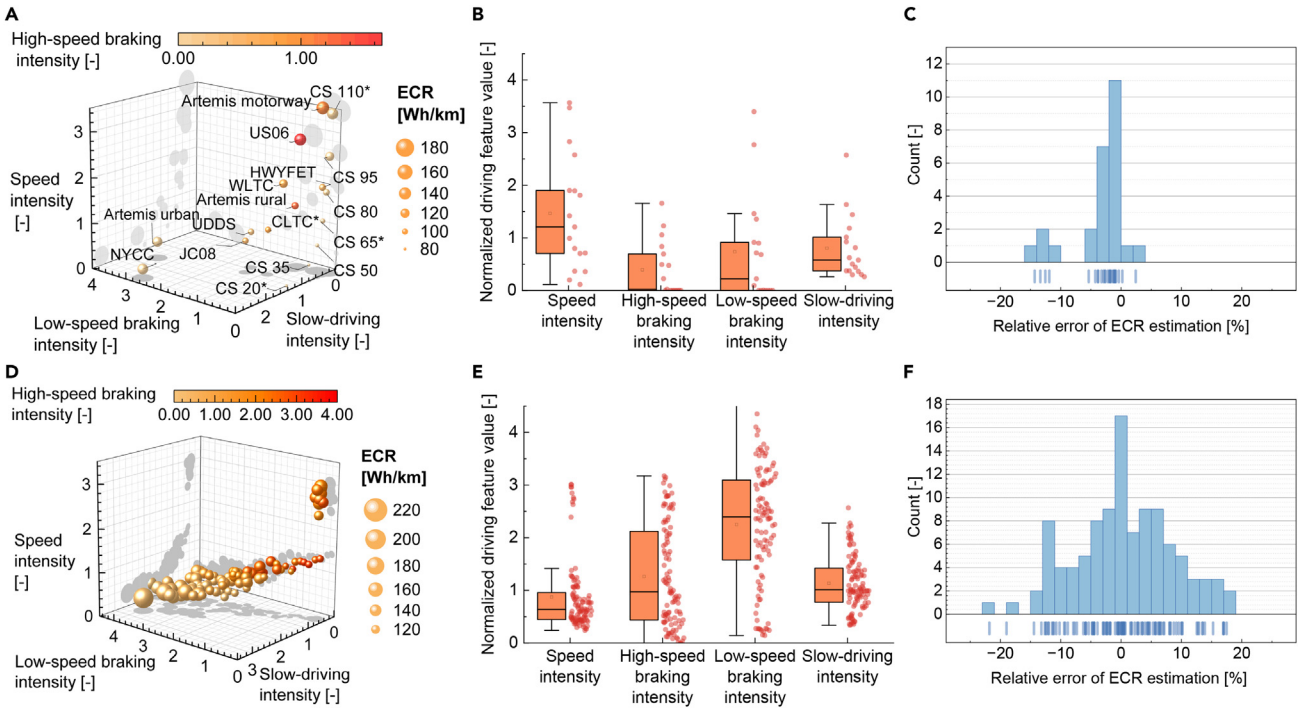

Figure 4. Driving feature distribution and ECR estimation results

(A) 3D distributions of driving features for laboratory test cycles. The x, y, and z axes represent the normalized low-speed braking intensity, slow-driving intensity, and speed intensity, respectively. The color scale represents the normalized high-speed braking intensity. Each ball represents a test cycle, and the size of the ball represents the measured ECR of the cycle.

(B) Boxplot of the driving feature distributions of the laboratory test cycles. The x axis is the driving features, the y axis is the normalized driving features (normalized based on the CLTC), the box limits represent the 25th and 75th percentiles, the center line represents the median, the whiskers represent the 1.5× interquartile range, and the red dots represent the data samples.

(C) Histogram of the estimation error of the GECRs for laboratory tests. The x axis is the relative estimation error, and the y axis is the number of test cycles.

(D) 3D driving feature distributions for real-world driving trips, similar to (A).

(E) Boxplot of the driving feature distributions of the real-world driving trips, similar to (B).

(F) Histogram of the estimation error of the GECRs for real-world trips, similar to (C).

include comprehensive driving, highway driving, aggressive driving, congested driving, and constant-speed driving conditions. Comprehensive driving cycles, such as the CLTC, urban dynamometer driving schedule (UDDS), and worldwide harmonized light-vehicle test cycle (WLTC), are distributed in the center of the feature space. Highway and aggressive driving cycles, such as the Artemis motorway test cycle, US06 test cycle, and highway fuel economy test (HWFET) cycles, are associated with higher speed intensities, and congested driving cycles, such as Artemis urban and New York City cycle (NYCC), are associated with low-speed braking intensities and slow-driving intensities. The CSSs exhibit opposite trends in terms of the speed and slow-driving intensity, with the braking intensity equal to zero. The distribution of the driving features from real-world driving tests is also visualized (Figures 4D and 4E and Note S7). The 3D distribution of results for real-world driving trips is very similar to that for laboratory tests, i.e., distributed from the lower left to upper right; however, the braking intensity and slow-driving intensity in real-world driving are significantly greater than those in standard test cycles, which is a common issue observed in many cities due to increased traffic congestion. These results further highlight the irrationality inherent in using a fixed driving cycle to represent a wide range of real-world driving conditions, as is common among existing standards. In summary, since various laboratory test cycles and real-world driving trips are used in our validation, the generalizability of the GECIs can be reliably evaluated.

Table 2. Metrics for the results of the training set and test sets

Metric	Training set (laboratory)	Test set (laboratory)	Test set[a] (real world)
RMSE (Wh/km)	1.87	8.30	13.56
MAPE (%)	1.47	3.84	7.12

[a]The ECR constant bias and elevation differences in real-world driving were compensated for (detailed in experimental procedures and Note S10).

Validation of the estimation performance

The GECRs were subsequently used to estimate the ECRs of the laboratory test cycles and real-world trips in the test set (the results are shown in Table 2). For the laboratory test, the MAPE of the 26 test cycles was 3.84%. Notably, the errors of most of the estimation results (Figures 4C and S1) were concentrated at approximately zero, except for those of the urban congestion cycles (the

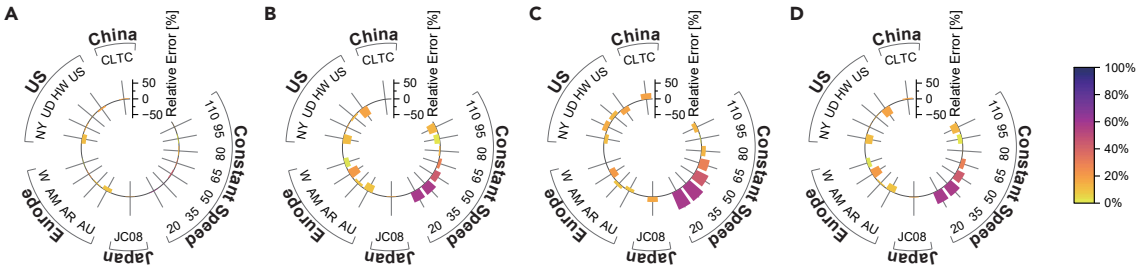

Figure 5. Comparison of the GECR results and the existing standards for estimating the ECRs of different driving cycles

(A) The GECRs, (B) the CLTC (used in China), (C) the WLTC (used in Europe), and (D) the combined ECRs from the UDDS and HWFET (used in the United States). Radial bar plots are used to show the adaptability of the evaluation indices, where 17 different driving cycles are distributed around the circles. The height of the bar represents the relative error in estimating the ECRs of the test cycles, namely the standardized test cycles in China, Europe, the United States, and Japan, and for CSSs. Due to space limitations, the test cycle names are shortened.

The full names of the test cycles are as follows: UD, UDDS; HW, HWFET; US, US06; NY, NYCC; W, WLTC; AM, Artemis motorway; AR, Artemis rural; and AU, Artemis urban. An outward-protruding error bar indicates that the estimated ECR is larger than the tested ECR, while an inward-protruding error bar indicates that the estimated ECR is smaller than the tested ECR.

Artemis urban cycle and NYCC). The MAPE was reduced to 2.17% when urban congestion cycles were excluded (the MAPE for 22 test cycles). This accuracy is extremely high because the uncertainty and measurement error in standard tests of a same test cycle often exceed 1%.[35] The estimation performance slightly deteriorates under traffic congestion conditions due to the high nonlinearity of low-speed braking energy consumption (Notes S3 and S4). For the real-world test cycles (Figures 4F and S2), the MAPE of the 106 real-world trips was 7.12%. Although the error was larger than that in the laboratory results, the GECRs still effectively characterize the real-world energy consumption of BEVs considering the impact of unobserved factors in the real world, such as the wind speed, road surface differences, steering variations, and driving-speed measurement error.

DISCUSSION

To further demonstrate the advantages of our method for evaluating the energy consumption of BEVs, we compare the accuracy and adaptability of the GECR-based paradigm with those of existing standards by using the results from our laboratory tests (Figure 5). There is a significant error when adapting the existing standards to other test cycles (Figures 5B–5D). The maximum relative error is approximately 50%, and the MAPEs based on the CLTC, WLTC, and US cycles are 17.1%, 20.5%, and 16.6%, respectively. Since test cycles represent different typical driving profiles, these results confirm that the existing standard BEV energy-consumption assessment methods are incapable of being adapted to diverse driving conditions. In contrast, the error for the GECRs is very small (Figure 5A), and the MAPE of the estimated ECRs for the 17 different driving cycles is only 3.3%, approximately five times less than that for the existing standards. This comparison further validates the significantly improved generalizability of the GECRs over the conventional standard evaluation approaches.

By decoupling the impact of the driving speed, the GECRs are approximately speed independent, allowing them to be adapted to various regions, time periods, and drivers. Moreover, obtainable through standard test procedures, GECRs hold significant potential for broad application across many BEV models and for providing publicly available BEV energy-consumption information, with profound significance for society, industry, and academia. Specifically, for society, awareness of BEV energy consumption will improve, which is crucial for reducing range anxiety, guiding eco-driving practices, and promoting the acceptance of BEVs. For industry, GECRs enable the interoperability of energy-consumption results among standard tests in different regions, as well as for real-world driving scenarios, exhibiting great potential for promoting the advanced regulation of BEV energy efficiency. Academically, GECRs provide a publicly available and easy-to-implement fundamental model for reliable BEV energy-consumption estimation. Consequently, scholars across diverse domains can readily gain insight into various BEV energy-consumption characteristics, enabling the utilization of specific traffic or driving behavior information to accurately estimate energy consumption for remaining range estimation[36]; infrastructure planning[37,38]; energy, carbon, or economic assessment[6–8,39]; and other tasks. On the other hand, the GECR model can be alternatively used to optimize speed profiles, such as to guide driving behavior,[40] further enhance route planning,[41] and optimize charging navigation.[42,43]

However, the results show that the GECRs slightly underestimate the energy consumption under extremely congested conditions due to the highly nonlinear energy consumption of low-speed braking. Nevertheless, because low-speed driving is associated with a short driving distance and limited total energy consumption, accurately estimating energy consumption in congested traffic situations is generally not critical for evaluating and predicting BEV energy consumption.[44] The sampling frequency might also affect the model accuracy. The sampling frequency in our experiments was 20 Hz due to the requirements of existing standards, which is sufficient for capturing vehicle speed dynamics. However, the sampling frequency of some real-world driving data collection projects is less than 0.1 Hz. At low sampling frequencies, the deceleration process may not be well captured during BEV braking, which may reduce the accuracy of brake-related energy-consumption estimation.

Ideally, all relevant factors, including temperature,[45] wind speed,[46] road surface conditions,[47] road slope,[48] battery aging,[49] etc., should be considered in energy-consumption evaluations.

However, this study focused primarily on the driving speed profile, since it is the focus of the current standards and represents the most crucial factor due to its highly dynamic and complex characteristics (discussed in Note S2). In many scenarios, such as the real-world trips in this paper, the impact of other factors is relatively constant and can be simply compensated for by an offset. Among these factors, temperature is an influential factor in addition to speed. While the complexity of the temperature model is relatively low, conducting temperature tests is notably time consuming and is beyond the scope of this paper.

Conclusion

In conclusion, we propose a data-driven approach that effectively balances standardizability and generalizability when evaluating the energy consumption of BEVs. This approach significantly reduces the discrepancies between standard testing and real-world driving. Through our experimental results, we demonstrate the great potential of GECRs for supporting accurate and generalizable standardized energy-consumption evaluations for various BEV models. This approach, in turn, is expected to promote the understanding and acceptance of BEVs for consumers while also providing a comprehensive and credible fundamental model for policymaking, scientific studies, and industrial applications. Additionally, our approach highlights the feasibility of using data-driven solutions to enhance the existing standards, enabling them to better reflect real-world characteristics.

EXPERIMENTAL PROCEDURES

Resource availability

Lead contact

Further information and requests for resources should be directed to the lead contact, Xinmei Yuan (yuan@jlu.edu.cn).

Materials availability

No new unique reagents were generated in this study.

Data and code availability

The data supporting the findings and the source code associated with this article are available at https://doi.org/10.6084/m9.figshare.23904102.[50]

Experimental setup

The laboratory test was performed with a 4WD chassis dynamometer (HORIBA VULCAN II EMS-CD48L 4WD Xcold). The DC discharged energy was measured with a four-channel power analyzer (Hioki PW3390 with AC/DC current probe CT6844-05). The DC energy consumption and driving speed were measured during the entire test procedure at a 20 Hz sampling frequency and synchronized over ethernet. The full AC recharged energy was also measured by a power analyzer to obtain the relationship between the AC and the DC energy consumption (Note S9). The laboratory test procedure was performed according to the corresponding test standards in China.[34] Dedicated drivers conducted driving tests according to the given speed profiles. The battery was charged by a slow charger.

A variant of the CLTC test was conducted to characterize the GECRs. The test included repeated CLTCs and CSSs of 110, 65, and 20 km/h (detailed in Note S5). The measured data were split into separate test cycles during postprocessing, where continuous measured data with speed errors less than ±1 km/h were captured for each CSS, and the high-SOC test data and data for the transitions between test cycles were discarded; as a result, separate CLTC and CSS datasets were obtained for GECR characterization. Other laboratory test cycles, such as UDDS, US06, HWFET, NYCC, WLTC, Artemis motorway, Artemis rural, Artemis urban, JC08 test cycles, and CSS at 35, 50, 80, and 95 km/h, with each cycle repeated twice, were employed for generalizability testing. The cycle tests and postprocessing steps were similar to those of the CLTC tests.

A real-world driving test was conducted in Changchun, China. DC energy consumption and driving speed were measured via a CAN bus with a sampling frequency of 20 Hz. As in the laboratory test, dedicated drivers followed road traffic on selected or random routes. Finally, 30 real-world driving trips on selected routes and 76 real-world driving trips on random routes were used, as shown in Figure 3 (detailed in Note S7).

GECR model

Our GECR model is expressed as follows:

$$\mathrm{ECR}_j = \mathbf{G\hat{E}CR}^{\mathrm{T}} \cdot \mathbf{I}_j, \quad \text{(Equation 1)}$$

where ECR_j is the ECR for driving cycle j and $\mathbf{G\hat{E}CR}$ is a five-dimensional coefficient vector representing the GECRs, which is expressed as:

$$\mathbf{G\hat{E}CR} = \left[\hat{G}_0, \hat{G}_{\mathrm{spd}}, \hat{G}_{\mathrm{hi\_brk}}, \hat{G}_{\mathrm{lo\_brk}}, \hat{G}_{\mathrm{slw}}\right]^{\mathrm{T}}, \quad \text{(Equation 2)}$$

where $\hat{G}_0, \hat{G}_{\mathrm{spd}}, \hat{G}_{\mathrm{hi\_brk}}, \hat{G}_{\mathrm{lo\_brk}}$, and $\hat{G}_{\mathrm{slw}}$ represent the ECR constant, speed sensitivity, high-speed braking sensitivity, low-speed braking sensitivity, and slow-driving sensitivity, respectively, and $\mathbf{I}_j$ is a five-dimensional driving feature vector for driving cycle j, which is represented as:

$$\mathbf{I}_j = \left[1, I_{\mathrm{spd},j}, I_{\mathrm{hi\_brk},j}, I_{\mathrm{lo\_brk},j}, I_{\mathrm{slw},j}\right]^{\mathrm{T}}, \quad \text{(Equation 3)}$$

where $I_{\mathrm{spd},j}, I_{\mathrm{hi\_brk},j}, I_{\mathrm{lo\_brk},j}$, and $I_{\mathrm{slw},j}$ are the speed intensity, high-speed braking intensity, low-speed braking intensity and slow-driving intensity, respectively. These variables can be calculated as:

$$I_{\mathrm{spd}}(\mathbf{V}) = \sum_{i=1}^{n-1} \bar{v}(i)^3 \Big/ \sum_{i=1}^{n-1} \bar{v}(i), \quad \text{(Equation 4)}$$

$$I_{\mathrm{hi\_brk}}(\mathbf{V}) = \sum_{\substack{i=1 \\ \bar{v}(i) \geq v_{\mathrm{th}}}}^{n-1} E_{\mathrm{brk}}(i) \Big/ t_s \sum_{i=1}^{n-1} \bar{v}(i), \quad \text{(Equation 5)}$$

$$I_{\mathrm{lo\_brk}}(\mathbf{V}) = \sum_{\substack{i=1 \\ \bar{v}(i) < v_{\mathrm{th}}}}^{n-1} E_{\mathrm{brk}}(i) \Big/ t_s \sum_{i=1}^{n-1} \bar{v}(i), \quad \text{(Equation 6)}$$

$$I_{\mathrm{slw}}(\mathbf{V}) = (n-1) \Big/ \sum_{i=1}^{n-1} \bar{v}(i) \quad \text{(Equation 7)}$$

where $\mathbf{V}$ is the set of driving speeds in a test cycle, n is the number of sampling points, t_s is the sampling period, and v_{th} is the threshold velocity for low- and high-speed driving, which is selected to be 15 km/h in this study according to Miri et al.[31] and Note S3. $\bar{v}$ is the average speed in a sampling period, and $E_{\mathrm{brk}}(i)$ is the braking energy in the i^{th} sampling period. The average speed in a sampling period is defined as:

$$\bar{v}(i) = \frac{v(i)+v(i+1)}{2}, \quad \text{(Equation 8)}$$

where $v(i)$ is the speed at the i^{th} sampling time. The braking energy in the i^{th} sampling period is expressed as:

$$E_{\mathrm{brk}}(i) = \begin{cases} 0 & \Delta E_{\mathrm{k}}'(i) \leq 0 \\ \Delta E_{\mathrm{k}}'(i) & \Delta E_{\mathrm{k}}'(i) > 0 \end{cases}, \quad \text{(Equation 9)}$$

where $\Delta E_{\mathrm{k}}'(i)$ is the kinetic energy change due to accelerating or braking. Assuming that the sampling period is small enough that the driving or braking state does not change within a sampling period, $\Delta E_{\mathrm{k}}'(i)$ can be approximated as:

$$\Delta E_{\mathrm{k}}' = \int_{t(i)}^{t(i)+t_s} \left(-m\frac{\mathrm{d}v(t)}{\mathrm{d}t} - A - Bv(t) - Cv(t)^2\right) v(t)\mathrm{d}t, \quad \text{(Equation 10)}$$

where m is the tested mass of the vehicle and A, B, C denote the road load coefficients from coastdown testing, also called the target coefficients in the United

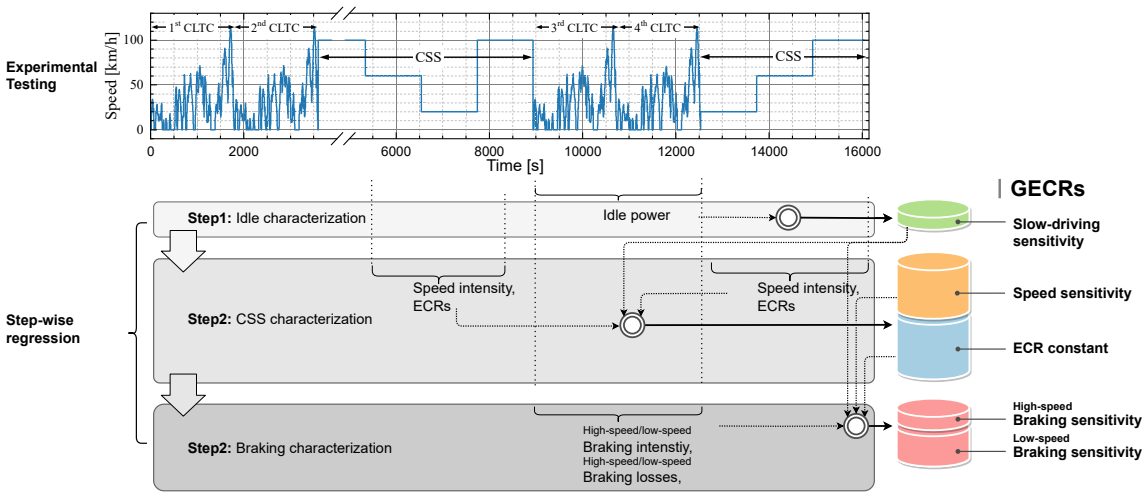

Figure 6. Schematic of the stepwise regression approach

At the top is the speed profile in the modified CLTC test. Curly brackets are used to mark the data segments used for the different steps, and the variables used for regression are denoted below the curly brackets. The cylinders of different colors represent the characterized GECRs, and the upper characterized indices are used to estimate the lower indices.

States. Using bilinear transform, the discrete form of Equation 10 can be approximated as:

$$\Delta E_k' = \frac{1}{2}m\left(v(i-1)^2 - v(i)^2\right) - \frac{A}{2}(v(i-1)+v(i))\Delta t - \frac{B}{3}\left(v(i-1)^2+v(i)^2+v(i-1)v(i)\right)\Delta t - \frac{C}{4}\left(v(i-1)^3+v(i-1)^2v(i)+v(i-1)v(i)^2+v(i)^3\right)\Delta t \quad \text{(Equation 11)}$$

By using the driving features of the speed profile in a standardized test cycle as the base values, all the features are normalized as:

$$I_{spd,j} = I_{spd}(\mathbf{V}_j) / I_{spd}(\mathbf{V}_{base}), \quad \text{(Equation 12)}$$

$$I_{hi\_brk,j} = I_{hi\_brk}(\mathbf{V}_j) / I_{hi\_brk}(\mathbf{V}_{base}), \quad \text{(Equation 13)}$$

$$I_{lo\_brk,j} = I_{lo\_brk}(\mathbf{V}_j) / I_{lo\_brk}(\mathbf{V}_{base}), \quad \text{(Equation 14)}$$

$$I_{slw,j} = I_{slw}(\mathbf{V}_j) / I_{slw}(\mathbf{V}_{base}), \quad \text{(Equation 15)}$$

where $\mathbf{V}_j$ is the set of driving speeds in the j^{th} test cycle and $\mathbf{V}_{base}$ is the set of driving speeds in the selected standardized cycle. As a result, the normalized driving features $\mathbf{I}_j$ are unitless, the units of GECRs are the same as those of the ECR, and the sum of the GECRs is approximately equal to the ECR of the CLTC.

Characterization procedures

Considering that the condition number of Equation 1 is large, which leads to unstable regression results, common linear least-squares methods are not suitable for characterizing GECRs. To solve this problem, a stepwise regression approach is proposed by leveraging the fact that some driving features are equal to zero under certain driving conditions; e.g., during idle periods, the speed intensity and braking intensity are equal to zero, and in a CSS, the braking intensity becomes zero. Three steps were applied in the characterization process, which is illustrated in Figure 6.

Step 1: idling characterization. All the idle segments in the CLTC are captured, and the mean idle power is calculated to characterize the slow-driving sensitivity of the tested BEV:

$$\hat{G}_{slw} = \overline{p}_{idle} \cdot I_{slw}(\mathbf{V}_{base}), \quad \text{(Equation 16)}$$

where $\overline{p}_{idle}$ is the mean idle power and $\mathbf{V}_{base}$ is obtained from the standard speed profile in the CLTC.[34]

Step 2: CSS characterization. Repeated CSSs at 110, 65, and 20 km/h are captured. The speed intensities and slow-driving intensities are calculated based on Equation 4 and Equation 7, respectively, and the braking intensities are assumed to be zero. The impact of the slow-driving intensity can be estimated using the result of Equation 16. Then, Equation 1 can be expressed as

$$\mathrm{ECR}_j - \hat{G}_{slw} \cdot I_{slw,j} = \hat{G}_0 + \hat{G}_{spd} \cdot I_{spd,j}. \quad \text{(Equation 17)}$$

A linear least-squares approach is applied to Equation 17 to obtain the ECR constant $\hat{G}_0$ and the speed sensitivity $\hat{G}_{spd}$.

Step 3: braking characterization. The braking losses in a sampling period are approximated as:

$$E_{brk}^{loss}(i) = \max(E_{brk}(i) + \min(\overline{p}_d(i)t_s, 0), 0), \quad \text{(Equation 18)}$$

where $\overline{p}_d(i)$ is the mean discharge power of the battery in the i^{th} sampling period; then, the braking losses in the high- and low-speed ranges can be calculated as:

$$E_{hi\_brk}^{loss}(\mathbf{V}) = \sum_{\substack{i=1 \\ \overline{v}(i) \geq v_{th}}}^{n-1} E_{brk}^{loss}(i), \quad \text{(Equation 19)}$$

$$E_{lo\_brk}^{loss}(\mathbf{V}) = \sum_{\substack{i=1 \\ \overline{v}(i) < v_{th}}}^{n-1} E_{brk}^{loss}(i). \quad \text{(Equation 20)}$$

Using the energy consumption model in Equation 1, the braking losses are approximately equal to the product of the braking sensitivity and braking intensity. The following equation applies when the low-speed braking loss is not zero:

$$\frac{E_{hi\_brk}^{loss}(\mathbf{V}_j)}{E_{lo\_brk}^{loss}(\mathbf{V}_j)} = \frac{\hat{G}_{hi\_brk} I_{hi\_brk,j}}{\hat{G}_{lo\_brk} I_{lo\_brk,j}}. \quad \text{(Equation 21)}$$

Table 3. List of abbreviations

Abbreviation	Definition
BEV	battery electric vehicle
ECR	energy-consumption rate
GECR	generalized energy-consumption rate
RMSE	root-mean-square error percentage
MAPE	mean absolute percentage error
CAN	controller area network
SOC	state of charge
Test cycle names	
CSS	constant-speed segments
CLTC	China light-duty vehicle test cycle
UDDS	urban dynamometer driving schedule developed by the US EPA
WLTC	worldwide harmonized light-vehicle test cycle
NYCC	New York City cycle
HWFET	highway fuel economy test cycle developed by the US EPA
Artemis	European assessment and reliability of transport emission models and inventory systems
US06	supplemental federal test procedure developed by the US EPA
JC08	Japan light-duty vehicle test cycle

The CLTC is split into three phases—slow, medium, and fast—according to its definition.[34] Phase 1 and phase 3 are used for characterizing braking intensities due to their typical low- and high-speed braking characteristics. Substituting the estimated $\hat{G}_c$, $\hat{G}_{spd}$, and $\hat{G}_{slw}$ values into Equation 1 yields:

$$\hat{G}_{hi\_brk} \cdot I_{hi\_brk,j} + \hat{G}_{lo\_brk} \cdot I_{lo\_brk,j} = ECR_j - \hat{G}_0 - \hat{G}_{slw} \cdot I_{slw,j} - \hat{G}_{spd} \cdot I_{spd,j}. \quad \text{(Equation 22)}$$

By substituting Equation 21 into Equation 22, the high-speed sensitivity $\hat{G}_{hi\_brk}$ and low-speed sensitivity $\hat{G}_{lo\_brk}$ can be obtained.

Because brake regenerative efficiency is the most nonlinear factor in the model, the proposed stepwise regression approach avoids the influence of uncertainty in brake regenerative efficiency on other terms, thereby achieving highly stable results.

Evaluation

We evaluated the generalizability of our approach by estimating the ECRs of the other 13 × 2 laboratory test cycles and 106 real-world driving trips using characterized GECRs. The ECRs of the laboratory test cycles and the real-world driving trips were estimated with Equation 1. However, due to the differences between laboratory test results and real-world driving environments, compensation for the ECRs of real-world driving trips estimated with Equation 1 was performed via the following equation:

$$ECR_R = \hat{E}CR + ECR_g + \hat{G}^{corr}_{const}, \quad \text{(Equation 23)}$$

where ECR_R is the estimated ECR of a real-world driving trip, $\hat{E}CR$ is the ECR estimated with Equation 1, and ECR_g estimates the impact of slope on the ECR, which is directly calculated as:

$$ECR_g = mg\Delta h, \quad \text{(Equation 24)}$$

where g is gravitational acceleration and Δh is the difference in elevation between the start and the endpoint of a trip. $\hat{G}^{corr}_{const}$ is the constant ECR bias in real-world driving and was estimated over N_R randomly selected trips using the following equation:

$$\hat{G}^{corr}_{const} = \frac{\sum_{i=1}^{N_R} (ECR_i - \hat{E}CR_i - ECR_{g,i})}{N_R}, \quad \text{(Equation 25)}$$

where 6 trips ($N_R = 6$) were randomly selected from the 106 trips in this study, and we performed 100 random selections to verify the stability of this compensation approach. A discussion is provided in Note S10.

Two metrics were chosen in this study to evaluate the performance of the proposed models.

The RMSE (root-mean-square error) is the standard deviation of the residuals. This variable reflects how far predictions fall from observations using Euclidean distances, as follows:

$$RMSE = \sqrt{\frac{1}{n}\sum_{i=1}^{n}(\hat{y}_i - y_i)^2}, \quad \text{(Equation 26)}$$

where n is the number of samples, $\hat{y}_i$ is the estimated value, and y_i is the observation.

The MAPE measures how accurate the estimation is as a percentage, as shown in Equation 27. It is the most widely used metric because it yields an intuitive interpretation of relative error:

$$MAPE = \frac{100\%}{n}\sum_{i=1}^{n}\left|\frac{\hat{y}_i - y_i}{y_i}\right|. \quad \text{(Equation 27)}$$

For a list of abbreviations used in this paper, please see Table 3.

SUPPLEMENTAL INFORMATION

Supplemental information can be found online at https://doi.org/10.1016/j.patter.2024.100950.

ACKNOWLEDGMENTS

This work was supported by the National Natural Science Foundation of China (grants 52272393 and 52122216). We thank L. Xie, Y. Gao, X. Zhang, X. Guan, and D. Zhang for discussions and Z. Zhao, L. Meng, M. Lv, Y. Shao, and J. Zhou for help with the experimental testing and data analysis. Any opinions, findings, conclusions, or recommendations expressed in this material are those of the authors and do not necessarily reflect the views of the government.

AUTHOR CONTRIBUTIONS

Conceptualization, X.Y. and L.L.; methodology, X.Y.; investigation, Y.M., B.B., and L.G.; writing – original draft, X.Y.; writing – review & editing, J.H. and Y. Liu; funding acquisition, X.Y.; resources, H.Z., Y.J., and L.S.; supervision, X.Y. and J.H.

DECLARATION OF INTERESTS

Jilin University is in the process of applying for a US patent, application no. 17/646803 (January 3, 2022), related to this work, and it lists X.Y. and B.B. as the inventors.

Received: September 6, 2023
Revised: January 3, 2024
Accepted: February 14, 2024
Published: March 8, 2024

REFERENCES

1. Ivanova, G., and Moreira, A.C. (2023). Antecedents of Electric Vehicle Purchase Intention from the Consumer's Perspective: A Systematic Literature Review. Sustainability *15*, 2878.

2. Hoekstra, A. (2019). The underestimated potential of battery electric vehicles to reduce emissions. Joule *3*, 1412–1414.
3. Hannula, I., and Reiner, D.M. (2019). Near-term potential of biofuels, electrofuels, and battery electric vehicles in decarbonizing road transport. Joule *3*, 2390–2402.
4. Xie, L., Singh, C., Mitter, S.K., Dahleh, M.A., and Oren, S.S. (2021). Toward carbon-neutral electricity and mobility: Is the grid infrastructure ready? Joule *5*, 1908–1913.
5. Isik, M., Dodder, R., and Kaplan, P.O. (2021). Transportation emissions scenarios for New York City under different carbon intensities of electricity and electric vehicle adoption rates. Nat. Energy *6*, 92–104.
6. Requia, W.J., Mohamed, M., Higgins, C.D., Arain, A., and Ferguson, M. (2018). How clean are electric vehicles? Evidence-based review of the effects of electric mobility on air pollutants, greenhouse gas emissions and human health. Atmos. Environ. *185*, 64–77.
7. Popovich, N.D., Rajagopal, D., Tasar, E., and Phadke, A. (2021). Economic, environmental and grid-resilience benefits of converting diesel trains to battery-electric. Nat. Energy *6*, 1017–1025.
8. Jenn, A. (2020). Emissions benefits of electric vehicles in Uber and Lyft ride-hailing services. Nat. Energy *5*, 520–525.
9. Klingenberg, H. (1978). Harmonization of Testing Procedures for Automotive Exhaust Gas. SAE Trans. *87*, 2514–2542.
10. Chen, K., Zhao, F., Liu, X., Hao, H., and Liu, Z. (2021). Impacts of the New Worldwide Light-Duty Test Procedure on Technology Effectiveness and China's Passenger Vehicle Fuel Consumption Regulations. Int. J. Environ. Res. Publ. Health *18*, 3199.
11. Sun, Z., Wen, Z., Zhao, X., Yang, Y., and Li, S. (2020). Real-World Driving Cycles Adaptability of Electric Vehicles. World Electric Vehicle Journal *11*, 19.
12. Hao, X., Wang, H., Lin, Z., and Ouyang, M. (2020). Seasonal effects on electric vehicle energy consumption and driving range: A case study on personal, taxi, and ridesharing vehicles. J. Clean. Prod. *249*, 119403.
13. Zhou, Y., Wen, R., Wang, H., and Cai, H. (2020). Optimal battery electric vehicles range: A study considering heterogeneous travel patterns, charging behaviors, and access to charging infrastructure. Energy *197*, 116945.
14. Herberz, M., Hahnel, U.J.J., and Brosch, T. (2022). Counteracting electric vehicle range concern with a scalable behavioural intervention. Nat. Energy *7*, 503–510.
15. Letmathe, P., and Suares, M. (2017). A consumer-oriented total cost of ownership model for different vehicle types in Germany. Transport. Res. Transport Environ. *57*, 314–335.
16. Desreveaux, A., Bouscayrol, A., Trigui, R., Hittinger, E., Castex, E., and Sirbu, G. (2023). Accurate energy consumption for comparison of climate change impact of thermal and electric vehicles. Energy *268*, 126637.
17. Zhang, S., Wu, Y., Liu, H., Huang, R., Un, P., Zhou, Y., Fu, L., and Hao, J. (2014). Real-world fuel consumption and CO2 (carbon dioxide) emissions by driving conditions for light-duty passenger vehicles in China. Energy *69*, 247–257.
18. Hao, H., Liu, Z., Zhao, F., Li, W., and Hang, W. (2015). Scenario analysis of energy consumption and greenhouse gas emissions from China's passenger vehicles. Energy *91*, 151–159.
19. Peng, T., Ou, X., and Yan, X. (2018). Development and application of an electric vehicles life-cycle energy consumption and greenhouse gas emissions analysis model. Chem. Eng. Res. Des. *131*, 699–708.
20. Needell, Z.A., McNerney, J., Chang, M.T., and Trancik, J.E. (2016). Potential for widespread electrification of personal vehicle travel in the United States. Nat. Energy *1*, 16112–16117.
21. Wei, W., Ramakrishnan, S., Needell, Z.A., and Trancik, J.E. (2021). Personal vehicle electrification and charging solutions for high-energy days. Nat. Energy *6*, 105–114.
22. Ahmed, M., Zheng, Y., Amine, A., Fathiannasab, H., and Chen, Z. (2021). The role of artificial intelligence in the mass adoption of electric vehicles. Joule *5*, 2296–2322.
23. Qi, X., Wu, G., Boriboonsomsin, K., and Barth, M.J. (2018). Data-driven decomposition analysis and estimation of link-level electric vehicle energy consumption under real-world traffic conditions. Transport. Res. Transport Environ. *64*, 36–52.
24. Jiménez, D., Hernández, S., Fraile-Ardanuy, J., Serrano, J., Fernández, R., and Álvarez, F. (2018). Modelling the Effect of Driving Events on Electrical Vehicle Energy Consumption Using Inertial Sensors in Smartphones. Energies *11*, 412.
25. Wei, H., He, C., Li, J., and Zhao, L. (2022). Online estimation of driving range for battery electric vehicles based on SOC-segmented actual driving cycle. J. Energy Storage *49*, 104091.
26. Ullah, I., Liu, K., Yamamoto, T., Zahid, M., and Jamal, A. (2021). Electric vehicle energy consumption prediction using stacked generalization: an ensemble learning approach. Int. J. Green Energy *18*, 896–909.
27. Zhang, J., Wang, Z., Liu, P., and Zhang, Z. (2020). Energy consumption analysis and prediction of electric vehicles based on real-world driving data. Appl. Energy *275*, 115408.
28. Yuan, X., Zhang, C., Hong, G., Huang, X., and Li, L. (2017). Method for evaluating the real-world driving energy consumptions of electric vehicles. Energy *141*, 1955–1968.
29. Whang, S.E., Roh, Y., Song, H., and Lee, J.-G. (2023). Data collection and quality challenges in deep learning: A data-centric ai perspective. The VLDB Journal *32*, 791–813.
30. Wu, D., Yang, J., Ahsan, M.U., and Wang, K. (2023). Classification of integers based on residue classes via modern deep learning algorithms. Patterns *4*, 100860.
31. Miri, I., Fotouhi, A., and Ewin, N. (2021). Electric vehicle energy consumption modelling and estimation—A case study. Int. J. Energy Res. *45*, 501–520.
32. European Commission (2017). Commission Regulation (EU) 2017/1151 of 1 June 2017 Supplementing Regulation (EC) No. 715/2007 of the European Parliament and of the Council on Type-Approval of Motor Vehicles with Respect to Emissions from Light Passenger and Commercial Vehicles (Euro 5 and Euro 6) and on Access to Vehicle Repair and Maintenance Information, Amending Directive 2007/46/EC of the European Parliament and of the Council, Commission Regulation (EC) No. 692/2008 and Commission Regulation (EU) No. 1230/2012 and Repealing Commission Regulation (EC) No. 692/2008 (Official Journal of the European Communities, L).
33. Light Duty Vehicle Performance and Economy Measure Committee (2021). Battery Electric Vehicle Energy Consumption and Range Test Procedure. SAE International.
34. China National Standardization Administration Commission (2021). Test Methods for Energy Consumption and Range of Electric Vehicles– Part 1: Light-Duty Vehicles (Standardization Administration of China).
35. Lairenlakpam, R., Lairenlakpam, R., Kumar, P., Kumar, P., Thakre, G.D., and Thakre, G.D. (2019). Experimental Investigation of Electric Vehicle Performance and Energy Consumption on Chassis Dynamometer Using Drive Cycle Analysis. SAE International Journal of Sustainable Transportation, Energy, Environment, & Policy *1*, 23–38.
36. Varga, B., Sagoian, A., and Mariasiu, F. (2019). Prediction of electric vehicle range: A comprehensive review of current issues and challenges. Energies *12*, 946.
37. Micari, S., Polimeni, A., Napoli, G., Andaloro, L., and Antonucci, V. (2017). Electric vehicle charging infrastructure planning in a road network. Renew. Sustain. Energy Rev. *80*, 98–108.
38. Metais, M.-O., Jouini, O., Perez, Y., Berrada, J., and Suomalainen, E. (2022). Too much or not enough? Planning electric vehicle charging infrastructure: A review of modeling options. Renew. Sustain. Energy Rev. *153*, 111719.
39. Chen, X., Liu, Y., Wang, Q., Lv, J., Wen, J., Chen, X., Kang, C., Cheng, S., and McElroy, M.B. (2021). Pathway toward carbon-neutral electrical systems in China by mid-century with negative CO2 abatement costs informed by high-resolution modeling. Joule *5*, 2715–2741.

40. Delnevo, G., Di Lena, P., Mirri, S., Prandi, C., and Salomoni, P. (2019). On combining Big Data and machine learning to support eco-driving behaviours. J. Big Data *6*, 15–64.

41. Basso, R., Kulcsár, B., Egardt, B., Lindroth, P., and Sanchez-Diaz, I. (2019). Energy consumption estimation integrated into the electric vehicle routing problem. Transport. Res. Transport Environ. *69*, 141–167.

42. Muratori, M. (2018). Impact of uncoordinated plug-in electric vehicle charging on residential power demand. Nat. Energy *3*, 193–201.

43. Sutherland, B.R. (2020). Reducing Emissions and Costs with Vehicle-to-Grid. Joule *4*, 1630–1632.

44. Yuan, X., He, J., Li, S., Li, L., Shi, S., and He, B. (2020). Can Electric Vehicles Meet Highway-Trip Requirements?: Exploration of the Real-World Impact on Highway Driving Range Derating. EEE. Ind. Electron. Mag. *14*, 6–19.

45. Kambly, K., and Bradley, T.H. (2015). Geographical and temporal differences in electric vehicle range due to cabin conditioning energy consumption. J. Power Sources *275*, 468–475.

46. Yi, Z., and Bauer, P.H. (2017). Effects of environmental factors on electric vehicle energy consumption: a sensitivity analysis. IET Electr. Syst. Transp. *7*, 3–13.

47. Ayevide, F.K., Kelouwani, S., Amamou, A., Kandidayeni, M., and Chaoui, H. (2022). Estimation of a battery electric vehicle output power and remaining driving range under subfreezing conditions. J. Energy Storage *55*, 105554.

48. Sagaama, I., Kchiche, A., Trojet, W., and Kamoun, F. (2020). Impact of Road Gradient on Electric Vehicle Energy Consumption in Real-World Driving. In International Conference on Advanced Information Networking and Applications, pp. 393–404.

49. Barcellona, S., and Piegari, L. (2020). Effect of current on cycle aging of lithium-ion batteries. J. Energy Storage *29*, 101310.

50. Yuan, X. (2024). Data and Code for Validating Generalized Energy Consumption Evaluation for BEVs. Figshare. https://doi.org/10.6084/m9.figshare.23904102.